Complex Adaptive Systems and the Threshold Effect: Views from the Natural and Social Sciences:
Papers from the AAAI Fall Symposium
(FS-09-03)

Timing the Delivery of Preterm Fetus: A Case Study Based on Computer Simulation

Tina Yu[1], **Tsung-Hong Chiu**[2], **Jeroen van den Wijngaard**[3]

T'sang-T'ang Hsieh[2], **Berend E. Weserhof**[3], **Enson Tseng**[4]

[1]Department of Computer Science, Memorial University of Newfoundland, St. Johns, NL, Canada
[2]Department of Obstetrics and Gynecology, Chang Gung Memorial Hospital, Taipei, Taiwan
[3]Department of Biomedical Engineering and Physics, Academic Medical Center, Amsterdam, Netherlands
[4]Department of Family Practice Residency, McLaren Regional Hospital, Flint, MI, USA

Abstract

The propagation of blood flow along the fetoplacental arterial system has been hypothesized to have a compensatory response to placental anomalies that may result in fetal stress. When the placenta generates increased resistance, the umbilical artery blood flow would decrease and in the worst scenario become absent, which will lead to fetal asphyxia and hypoxia. To compensate for the decreased oxygen supply from maternal placenta, the fetal middle cerebral arteries would become dilated leading to an increased diastolic flow, hence more oxygen. This compensatory phase , however, only lasts for a certain period of time, after which the hypoxia may lead to fetal demise or long term irreversible organ damages. In high-risk pregnancies, Doppler ultrasound technology is commonly used to monitor the fetoplacental arterial blood flow to assess fetal well being. If the anomalies occur prior to the end of the 40-week of gestation, surgical or aggressive medical intervention might be necessary to save the fetal life. Timing this intervention, however, is complex due to the fine balancing act to minimize potential risks from prematurity and organ damage vs. rescuing a fetal life through cesarean section or aggressive medical treatment or natural delivery at the earliest possible gestational age. A reasonable goal is to allow the pregnancy to continue to the point just before fetal damage occurs. To achieve that goal, various testing criteria, e.g. venous Doppler and fetal heart rate, have been used to identify de-compensation. In this work, we conducted computer simulation of the fetoplacental arterial blood flow of a Systemic Lupus Erythematosus (SLE) pregnancy based on Doppler blood flow readings taken during the 10-day period prior to the delivery. The simulation suggests that timing the delivery based on either Doppler waveform readings or fetal heart rates give similar pregnancy outcome.

1. Introduction

The management of high-risk pregnancies due to placental disease relies on careful monitoring of the fetal well-being during the pregnancies. Normally, fetal biophysical profile, such as amniotic fluid volume and heart rate, and Doppler velocimetry are examined regularly to assess for fetal distress. When one or more of the readings are outside the normal range, proper interventions are taken to preserve fetal life.

The proposed pathophysiology of high-risk pregnancies due to placental disease is that the placenta generates increased resistance, indicated by increased umbilical artery (UA) Doppler waveforms, which lead to placental respiratory failure and fetal hypoxemia (Giles, Trudinger, and Baird 1985). This, in turn, triggers the compensatory hemodynamic changes, which redistribute blood flow towards essential fetal organs (brain, heart and adrenal glands) at the expense of the secondary organ systems (lungs, kidneys and bowel) (Waldimiroff et al. 1987). The duration of the compensatory phase varies, from days to weeks. When these compensatory mechanisms reach their maximum limit, myocardial dysfunction occurs (Reed et al. 1990). Once the disease enters this de-compensatory phase, the fetus is at high risk of dying and organ failure.

In obstetric practice, delivery is undertaken when the fetus shows signs of de-compensation. The choice of test to identify de-compensation, however, varies. Some clinicians use venous Doppler information to determine the time of delivery (Pardi et al. 1993) while others analyze biophysical profile (fetal heart rate and amniotic fluid volume) for evaluation (Vintzileos, Campbell, and Rodis 1989). One recent study observed that more than 50 % of fetuses delivered because of abnormal fetal heart rate did not have venous Doppler abnormalities (Ferrazzi et al. 2002). Another study reported that deterioration of the fetal arterial and venous systems occurred before an abnormal biophysical profile score in most cases but the time interval between the two was only 24 hours (Baschat, Gembruch, and Harman 2001). The reason behind these different compensatory fetal responses is not clear.

In (Romero, Kalache, and Kadar 2002), the authors conjectured that fetuses with more severe disease would develop abnormal venous Doppler, in addition to the abnormal biophysical profile readings. Timing the delivery based on venous Doppler will improve the outcome. One way to investigate this hypothesis is by examining the relationship be-

tween venous Doppler and fetal heart rates in compensatory fetuses.

In a previous work, (van den Wijngaard et al. 2006) reported that the variation of fetal heart rate will influence the Doppler blood flow resistance indices, based on the computer simulation of a fetal circulation model they developed. However, it assumes the fetus is not in compensatory condition; hence all model parameters are constant except the fetal heart rate. A compensatory fetus normally has an increased placental resistance (that trigged the compensation phase) and variable brain resistance (due to the dilated cerebral arteries for blood redistribution). Consequently, the dynamics of the fetal circulation is different.

This work expands that work by adopting an inverse modeling approach to study the correlation between venous Doppler and heart rate of a compensatory fetus. We used the Doppler blood flow data of a preterm fetus delivered at 28 weeks of gestation as the modeling target. The Doppler examinations were performed over the 10-day compensation period until the time of the delivery.

The paper is organized as follows. Section 2 gives a brief introduction to Doppler ultrasound technology. Section 3 describes a mathematical model of fetal arterial system. In Section 4, we explain the inverse modeling approach and the genetic algorithm implemented to carry out the inversion task. Meanwhile, the Doppler ultrasound data are described. Section 5 presents the modeling results, while Section 6 gives discussion. Finally, Section 7 concludes the paper.

2. Doppler Ultrasound and Blood Flow

The present-day Doppler ultrasound technology is based on the phenomenon that the frequency of light waves changes according to whether the light source is moving toward or away from the observer (Eden 1992). This Doppler Effect was named after the Austrian mathematician Christian Johann Doppler who discovered this phenomenon in 1842.

Doppler Effect can be used to record blood flow velocities in the fetoplacental arteries system. When the sound waves emitted from an ultrasound transmitter at a specific frequency encounter moving corpuscular elements in the blood, a frequency shift would occur and reflect back to an ultrasound receiver. Based on the frequency shift, the blood flow velocity can be calculated using the Doppler equation. The calculated velocities are normally displayed on the ultrasound monitor as amplitude traces (see Figure 1). For obstetric diagnosis, Doppler waveforms are used to measure blood flow resistances to help determining fetal well-being (Merz 2004).

The 3 most commonly used blood flow resistance indices are: Resistance Index (RI), Systolic/Diastolic (S/D) ratio and Pulsatility Index (PI). Their calculation is described in Figure 1. The PI takes slightly longer to calculate than the RI or S/D ratio because of the need to measure the mean height of the waveform. It does, however, give a broader range of values. For instance, when the end-diastolic flow (D) is absent or has a reverse flow, S/D cannot be measured while RI=1. PI is more useful in this case.

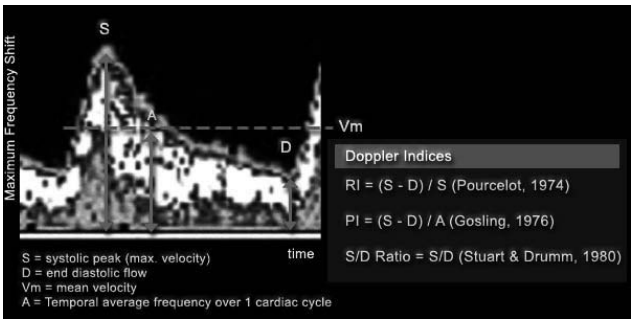

Figure 1: Doppler waveforms and flow velocity indices.

During the course of a pregnancy, the exchange of gas and nutrients in the placenta occurs partly through passive diffusion and partly through active transport processes. The oxygen- and nutrient-enriched blood enters the fetal circulation from the placenta via the umbilical vein. Doppler sampling of the two umbilical arteries is therefore the simplest examination of the fetal condition.

In a normal pregnancy, the end-diastolic flow velocity (D) in the umbilical artery (UA) increases in relation to the systolic velocity (S). As a result, the resistance indices PI and RI decline with advancing gestational age. Figure 2 gives the reference ranges of PI in the UA for different gestational ages, based on (Ebbing, Rasmussen, and Kiserud 2007).

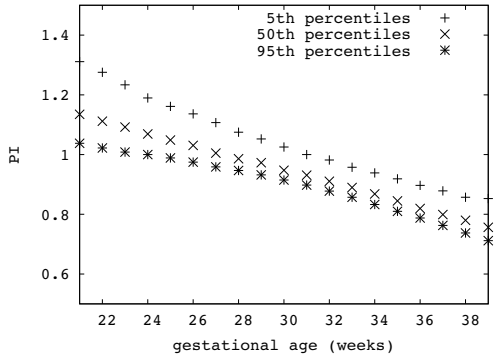

Figure 2: Reference ranges of PI in the umbilical artery.

Abnormal UA waveforms can occur due to the increased placenta resistance, which increased the impedance in the umbilical cord arteries. As a result, the end-diastolic flow (D) is decreased or become absent or reversed. Figure 3 shows the normal and abnormal UA waveforms based on the classification in (Marsal et al. 1987)

The middle cerebral artery (MCA) is another vessel that is frequently selected for Doppler scanning because its position makes the scanning easy with good reproducible results, hence a reliable source to assess fatal condition. As shown in Figure 4, the reference curve for the PI in the MCA has a typical parabolic shape with a maximum between 25 and 30 weeks' gestation (Ebbing, Rasmussen, and Kiserud 2007). A physiolologic decline in the resistance indices occurs dur-

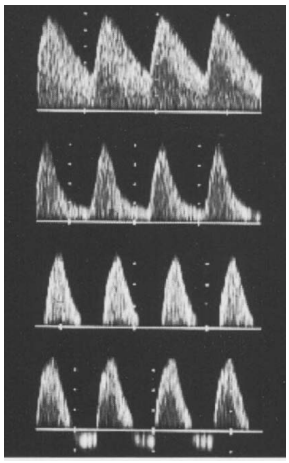

(a)Normal umbilical artery waveform

(b) Decreased end-diastolic flow

(c) Absent end-diastolic flow (AEDF)

(d) Reverse flow

Figure 3: Normal and abnormal umbilical artery waveforms.

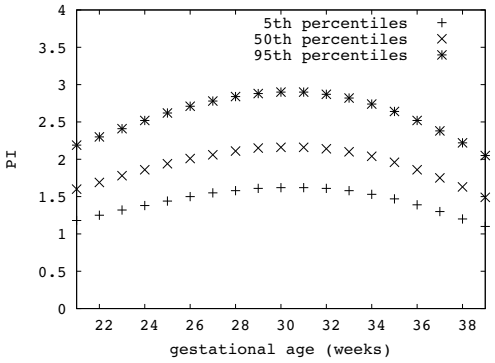

Figure 4: Reference ranges of PI in the middle cerebral artery.

ing the closing weeks of pregnancy.

Unlike UA, abnormal MCA waveforms are characterized by high diastolic flow velocities (D) (see Figure 5), hence with decreased PI. This phenomenon, called the brain-sparing effect, is explained in the next subsection.

2.1 Brain-Sparing Effect

Brain-sparing effect is a compensatory mechanism where the cerebral vessels become dilated due to the fetal hypoxemia, to increase the blood flow to the brain (Woo, et al). With the increased diastolic flow (D), the resistance indices of the cerebral arteries are decreased.

This hypoxemia-induce redistribution of blood volume in favor of the brain is a protective mechanism aimed at maintaining an adequate cerebral blood supply. The length of this compensatory phase varies from days to weeks. When the mechanism is no longer working, severe hypoxemia and academia would induce a state of general circulatory collapse leading to a loss of cerebral auto-regulation. The decompensation of cerebral hemodynamics can lead to severe brain damage and fetal death.

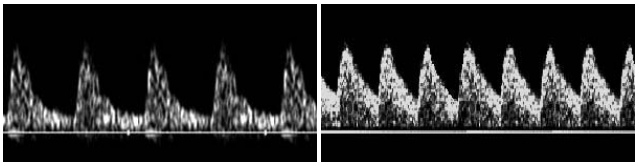

Figure 5: Normal (left) and abnormal (right) MCA waveforms.

3. The Fetoplacental Arterial System Model

We adopted the mathematical model developed by (Van den Wijngaard, 2006) to conduct our research. In this model, arterial flow waves are calculated at 8 different arterial locations (see Figure 6) from which their pulsality indices (PIs) can be estimated.

In (Van den Wijngaard, 2006), several model parameters were adjusted independently to evaluated their individual impact on the overall blood flow. They reported that increasing placental resistance would increase the PI in the UA but decrease the PI in the MCA. Similar results were observed when the brain resistance was decreased. Moreover, the increase or decrease of fetal heart rate decrease or increase the PIs in all arteries. One assumption they made was that the fetus was in a non-compensatory condition, where all model parameters were constant except the investigated individual parameter, which was varied in a systematic manner. A compensatory fetus has more than one parameters varied simultaneously as the result of the blood redistribution. Consequently, the dynamics of the fetal circulation will be different. To simulate the blood flow of a compensatory fetus, it requires tedious experimental design of different variations of the model parameters. Alternatively, we can adopt an inverse modeling approach to conduct the simulation. This approach is described in the following section.

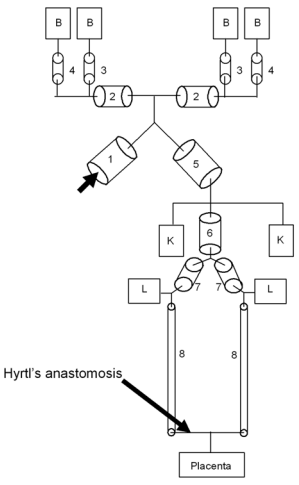

1. Ascending Aorta (Asc Ao)
2. (left and right) Carotid Arteries (Car As)
3. (left and right) Middle Cerebral Arteries (MCAs)
4. (left and right) Anterior Cerebral Arteries (ACAs)
5. Thoracic Aorta (Thor Ao)
6. Abdominal Aorta (Abdo Ao)
7. (left and right) Iliac Arteries (Iliac As)
8. Two Umbilical Arteries (UAs)

Figure 6: Overview of the fetoplacental arterial system.

4. Genetic Algorithms for Inverse Modeling

In inverse modeling, the model is a black box with unknown characteristic values. Given a set of outputs, the task is to identify these unknown characteristic values that produce outputs that match the given output to complete the model (see Figure 7). Recently, inverse modeling has been applied to study human pathophysiology (Bates, 2009).

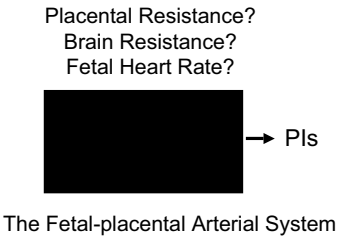

Figure 7: Inverse Modeling.

In our case, we have collected a series of PI data calculated from the Doppler waveforms of a compensatory fetus during the 10-day period prior to its delivery. The inversion task is to identify the corresponding parameter values in the fetal-placental artery system to produce blood flow that match these Doppler PIs. In particular, we are interested in the values of the fetal heart rate, the placental and brain resistances which have impact on the blood flow. Based on the information, we can analyze the correlation between fetal heart rate and blood flow in the compensatory fetus.

Inverse modeling has no unique solutions. In other words, there are multiple combinations of model parameter values that can produce the same blood flows (PIs). We therefore made multiple simulation runs and use the trend of parameter value variation (instead of the actual values) to give our interpretation.

4.1 The Patient Data

The patient was 30 years old with Systemic Lupus Erythematosus (SLE) and secondary antiphospholipid (APS) syndrome. Previously, she had two pregnancies but both of them were terminated prematurely due to medical condition. In this third pregnancy, Doppler ultrasound was examined frequently to monitor the fetal development.

The pregnancy went well until the 27th week when abnormal blood flows were observed: the UA had decreased end-diastolic flow while the MCA had increased end-diastolic flow (see Figure 8). The contraction stress test (CST) in Figure 9 showed late deceleration, indicating that the placenta may not be delivering adequate amount of oxygen to the fetus. The patient was admitted to the hospital for close observation.

The end-diastolic flow of UA continued to decrease until the 5th day when it became absent (AEDF). Meanwhile, the end-diastolic flow of MCA continued to increase (see Figure 10). Meanwhile, in addition to the late deceleration, the CST showed decreased heart rate variability (see Figure 11). This suggested that the cerebral vessels had become dilated, a result of brain-sparing effect.

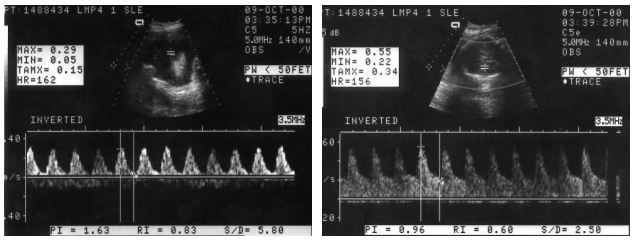

Figure 8: The Doppler UA (left) and MCA (right) at 27 weeks+2 days of gestation.

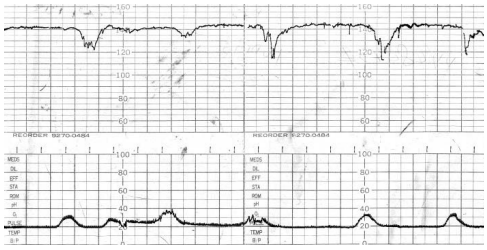

Figure 9: The CST of fetal heart rate at 27 weeks+2 days of gestation.

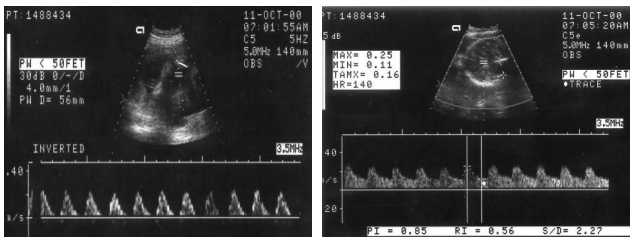

Figure 10: The Doppler UA (left) and MCA (right) at 27 weeks+5 days of gestation.

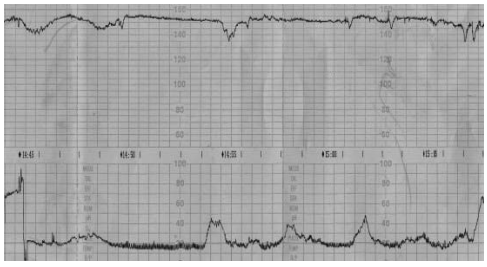

Figure 11: The CST of fetal heart rate at 27 weeks+5 days of gestation.

The similar flow pattern continued for another 5 days. At the gestational age of 28 weeks and 2 days, the UA end-diastolic flow became reversed. Meanwhile, the MCA flow was disappearing. This suggested that the fetus was at a decompensatory phase and the fetus was at high risk of organ failure and death. A cesarean section was immediately arranged to deliver the fetus. The newborn was a boy weighted 842 grams and had no anomalies.

Between 24 and 28 weeks' gestation, 8 Doppler ultrasound examinations were performed. Among them, 4 UA waveforms have AEDF and no PI values. The other 4 Doppler UA and MCA waveforms have calculated PIs which are shown in Figure 12. We will use this data set to inverse fetal heart rate and placental and brain resistance in the fetal-placental model. The inverse algorithm is a genetic algorithm, which is explained in the following subsection.

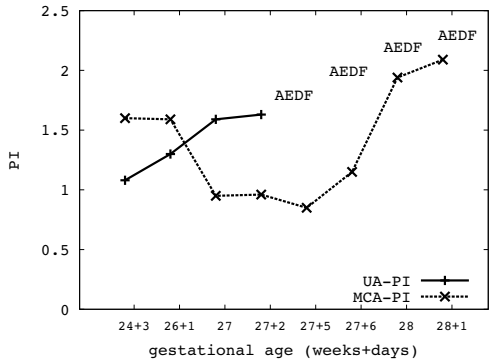

Figure 12: The Doppler UA and MCA PIs data series.

4.2 The Genetic Algorithm Implementation

Genetic Algorithms (GA) (Holland 1975) belong to the field of Evolutionary Computation which mimics the process of natural evolution for problem solving. In nature, individuals adapt to their environments to survive. Those who continue to exist are said to be fitter than those who have become extinct. In problem solving, fitter solutions will continue to exist among a population of possible solutions. As the evolution progresses, the population, in general, becomes fitter and fitter in its ability to solve the given problem. This approach of evolving problem solutions has been shown to be effective in many application areas.

Figure 13 gives the high-level flow of a genetic algorithm. Initially, a population of solutions is randomly generated. Each solution is then evaluated with its ability to solve the given problem and assigned with a fitness value. Those with better fitness are selected as parents to produce offspring using variation operations, such as crossover and mutation. The offspring then form a new generation. This evaluation-selection-variation cycle is repeated for many generations until the termination criterion is met. At the end of the process, the fittest individual is selected as the final solution to the given problem.

For our inverse problem, the solution is the fetal heart rate, placental and brain resistance values in the fetoplacental arterial system model that produce the blood flow matching the Doppler PIs. Since there are 8 Doppler screening, each has a heart rate, a placental and a brain resistance values, we used a vector of 24 real numbers to represent a solution.

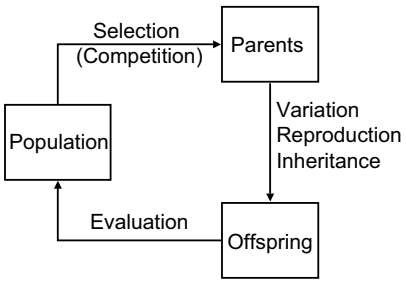

Figure 13: The high-level flow of genetic algorithms.

$R_{placenta_1}$	R_{brain_1}	FHR_1	·	·	·	·

Each value in the vector is the ratio between the fetal-placental model parameter value and the normal parameter value:

$$R_{placenta} = Resistance^{model}_{placenta} / Resistance^{normal}_{placenta}$$

$$R_{brain} = Resistance^{model}_{brain} / Resistance^{normal}_{brain}$$

$$FHR = HeartRate^{model}_{fetal} / HeartRate^{normal}_{fetal}$$

Note that the normal fetal heart rate and resistances values have been adjusted according to the fetal gestational age. Also, the range of $R_{placenta}$ is between 0.5 and 5, which represent the lower and upper limits of the physiological range (Adamson et al. 1990). The R_{brain} is between 0.2 and 1.5, which was chosen arbitrarily as the maximal decrease in brain resistance in the human fetus is not known. The FHR is between 0.5 and 1.5.

The fitness of a solution (F) is defined as the sum of the mismatch between the Doppler PIs and the PIs generated from the fetoplacental model based on the solution. For the UA with AEDF and no PI data, the mismatch is measured by the distance of its end-diastolic flow away from 0, since AEDF has end- diastolic flow velocity 0. The smaller the F is the fitter the solution is.

$$F = \sum_{i=1}^{8} abs(PI^{MCA}_{simulated_i} - PI^{MCA}_{Doppler_i}) + PI^{UA}_{mismatch_i}$$

$$PI^{UA}_{mismatch} = \begin{cases} abs(endDiastolicFlow_{simulated}), & \text{AEDF} \\ abs(PI^{UA}_{simulated} - PI^{UA}_{Doppler}), & \text{otherwise} \end{cases}$$

We implemented a tournament selection of size 2 to select solutions for reproduction. Two solutions in the population are randomly picked and compared. The one with a smaller F is the winner to participate in reproduction.

Two operators were implemented to produce offspring. In one-point crossover, two winning solutions are aligned and a crossover location is randomly selected. The sub-string in one solution is swapped with the substring in another solution to generate two offspring (see Figure 14).

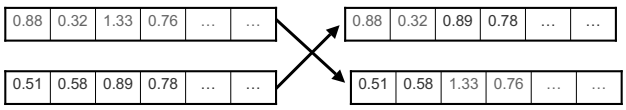

Figure 14: An example of one-point crossover.

The Gaussian mutation operator replaces the value in a cell with a new value. Assuming the current FHR_2 is v. The mutated value $v' = v + m$, where m is selected from the Gaussian distribution of 0 mean and standard deviation of 1.

Each value in the vector has probability of p_m to be mutated. Figure 15 describes this operation.

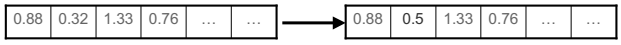

Figure 15: An example of Gaussian mutation.

The GA is implemented in Mathematica using the code from (Jacob 2001). The pseudo code of the implemented GA is given in Figure 16. We made 5 simulation runs using population size of 10, p_c=0.5, p_m=0.1. Each run lasts for 100 generations.

```
Begin GA
   g:=0  { generation counter }
   Initialize population P(g)
   Evaluate population P(g) {compute fitness values}
   While not done do
      g:=g+1
      If (rnd()> p_c)
            Select two individuals from P(g-1) for
            crossover and add offspring to P(g)
      Else
            Select one individual from P(g-1) for
            Gaussian mutation and add offspring to P(g)
      Evaluate P(g)
   End while
End GA
```

Figure 16: The implemented GA in pseudo code.

5. Results and Analysis

Figure 17 gives the UA PIs simulated by the fetoplacental model using the $R_{placenta}$, R_{brain} and FHR evolved by the 5 GA runs. The first 4 simulated UA PIs match the Doppler data in Figure 12 well. The other 4 Doppler waveforms are AEDF with no PI to match. Using the 0 end-diastolic flow as the target, the GA evolved model parameter values that give UA end-diastolic flow close to 0, which resembles AEDF (see Figure 24 to 27). The simulated UA PIs, however, have a wider range of values than the range of the first 4 simulated UA PIs. Nevertheless, they all have a similar increasing trend.

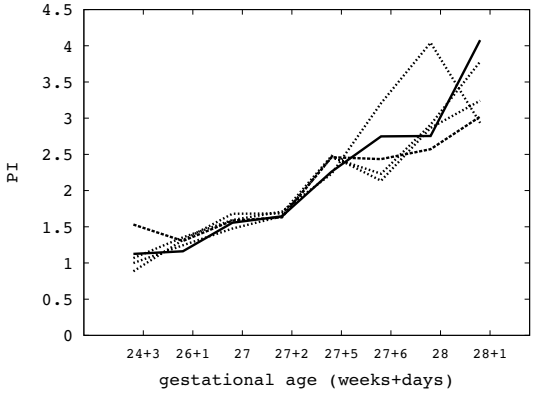

Figure 17: Simulated UA PI based on GA evolved model parameters.

Figure 18 gives the MCA PIs simulated by the fetoplacental model using the $R_{placenta}$, R_{brain} and FHR evolved by the 5 GA runs. The simulated MCA PIs match the Doppler data in Figure 12 very well. The mismatch of the simulated and the Doppler PIs is between 0.1 and 0.001. We will use the GA evolved model parameter values to interpret the blood circulation in the studied compensatory fetus.

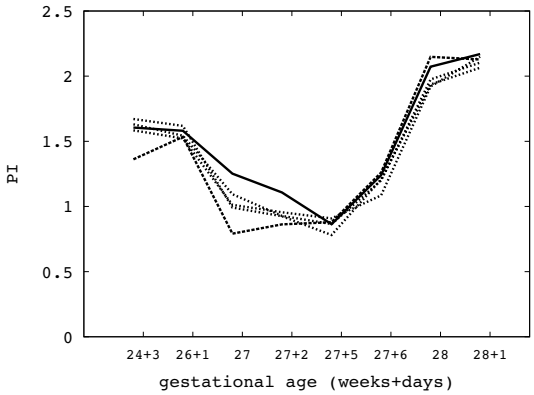

Figure 18: Simulated MCA PI based on GA evolved model parameters.

Figure 19 shows the $R_{placenta}$ values evolved by the 5 GA runs. It shows that the placental resistance starts to increase

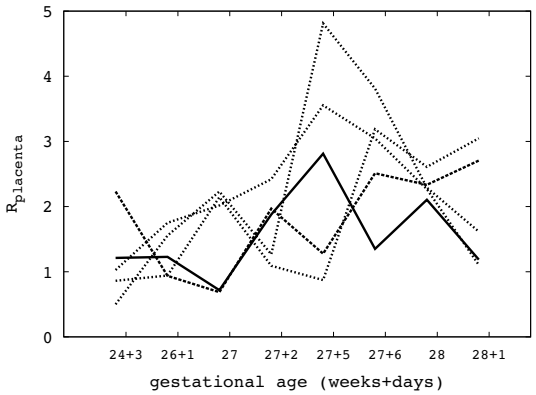

Figure 19: Placental resistance ($R_{placenta}$) evolved by the 5 GA runs.

either on the day of the 27 week of gestation or two day after the 27 weeks of gestation. After that, the resistance went up and down but with a general increasing trend.

The brain resistance R_{brain} decreased on the 27 week of gestation (see Figure 20). After that, the resistance decreased and increased with a trend similar to the PIs in the MCA (Figure 18).

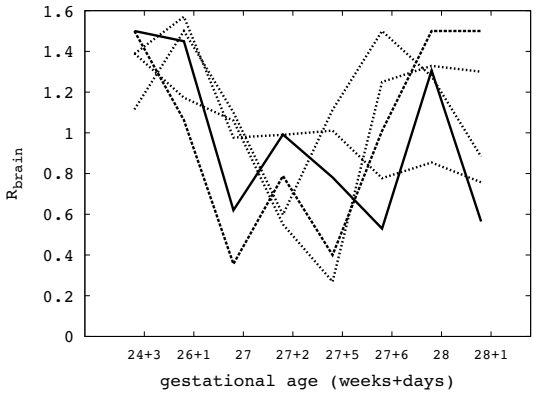

Figure 20: Brain resistance (R_{brain})evolved by the 5 GA runs.

The fetal heart rates (FHR) also had up and down but with a general trend of gradually decreasing. The heart rate reached the lowest point on the day before the fetus was delivered (see Figure 21).

These results suggest that in this patient case, fetal heart rate, placental and brain resistance have impact on the UA and MCA blood flow in the compensatory fetus. An increased PI in the UA can be caused by any combination of 1) the increase of placental resistance 2) the decrease of brain resistance 3) the decrease of heart rate. While an increased PI in the MCA can result from any combination of 1) the decrease of placental resistance 2) the increase of brain resistance. The impact of fetal heart rate on the PI in the MCA is not very clear.

We also used the $R_{placenta}$, R_{brain} and FHR evolved

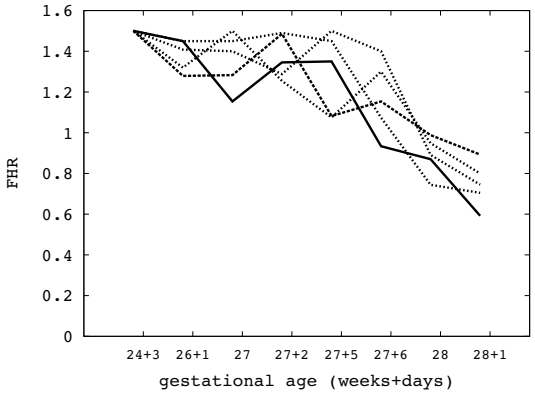

Figure 21: Fetal heart rate (FHR) evolved by the 5 GA runs.

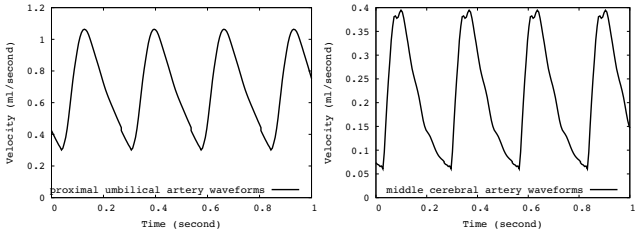

Figure 22: Simulated blood flow (24 weeks+3 days).

from one GA run to simulate the blood flow in the UA and the MCA (see Figures 22 - 27) of the fetal model.

The simulated fetal UA and MCA waveforms at the 24 week and 3 days of gestation (Figure 22) are normal (see Figure 3 (a) and Figure 5 (left)). However, two days after 27 weeks of gestation, the simulated waveforms (Figure 23) shows decreased end-diastolic flow in the UA. Meanwhile, the end-diastolic flow in the MCA is increased. They correspond to the Doppler waveforms shown in Figure 8.

The simulated fetal blood flow on the 27 week and 5 days of gestation (Figure 24) shows absent end-diastolic flow in the UA (AEDF). Meanwhile, the end-diastolic flow in the MCA continues to increase. They correspond to the Doppler waveforms shown in Figure 10.

Figure 25 to 27 give the simulated fetal blood flow on the last 3 day before the fetus was delivered. The UA shows sign of reverse flow while the MCA has increased end-diastolic flow (D), hence gives increased PI (see Figure 12). Also there is a visible heart rate decrease and low variation (indicated by the low waveform frequency). On the day before the delivery, the heart rate is about 60% of the normal rate at 107 beats per minute.

6. Discussion

Systemic lupus erythematosus (SLE) is associated with multiple adverse pregnancy outcomes, such as premature birth and fetal loss (Clowse et al. 2006). Currently, the pathophysiology of the disease activity during pregnancy remains unknown (cite). When the disease worsens during a preg-

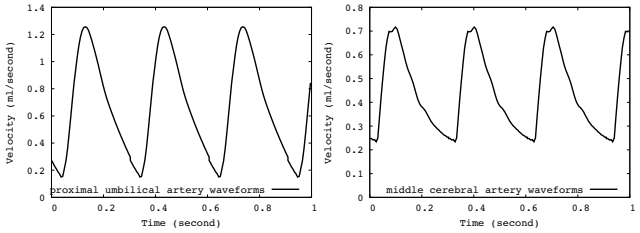

Figure 23: Simulated blood flow (27 weeks+2 days).

nancy, there is no effective treatment except delivery. This case study suggests that timing the delivery based on either venous Doppler readings or fetal heart rates give similar pregnancy outcome.

When the abnormalities of PI in the UA and in the MCA occurred (27 weeks and 5 days of gestational age), the fetal heart rate (FHR) also showed reduced variation and late deceleration. Both are signs of fetal hypoxemia. As the PI in the UA continued to increase, the FHR variation also decreased. Extremely low short term variation of FHR has been found to be a reliable predictor of metabolic academia at delivery or intrauterine death (Street et al. 1991). The day before the delivery, the FHR had less than 2 episodes of accelerations, which is the sign of de-compensation (Guzman et al. 1996). This timing result is similar to that based on the Doppler reverse flow in the UA.

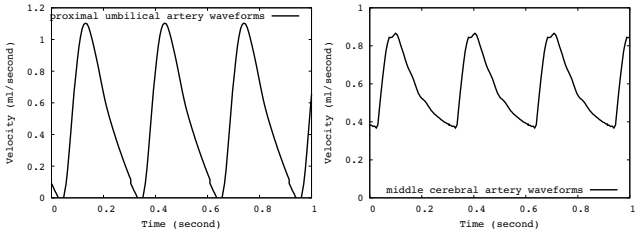

Figure 24: Simulated blood flow (27 weeks+5 days).

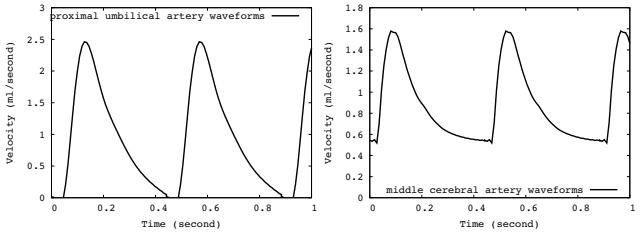

Figure 25: Simulated blood flow (27 weeks+6 days).

7. Conclusion

The propagation of blood flow and pressure along the fetal arterial tree is a complex system that is influenced by the interactions of many components. Currently, these interactions are not completely understood. While most researchers applied statistics to interpret compensatory fetal

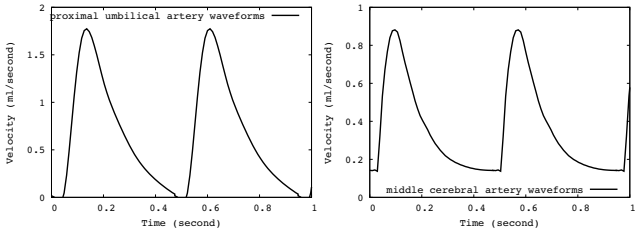

Figure 26: Simulated blood flow (28 weeks).

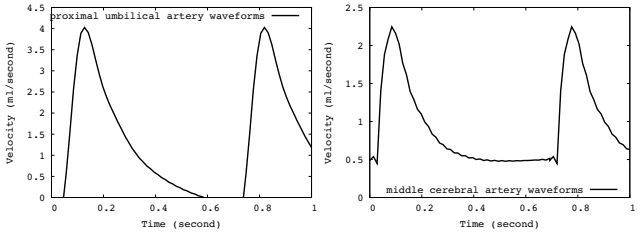

Figure 27: Simulated blood flow (28 weeks+1 days).

responses to suggest protocol for high-risk pregnancy management, the inverse modeling of fetal circulation is an alternative to study the interaction dynamics. This work applied a genetic algorithm to inverse placental and brain resistances and fetal heart rate based on the Doppler waveforms data of a compensatory fetus. The study suggests that in this SLE pregnancy case, venous Doppler and fetal heart rate abnormalities occurred simultaneously. Timing the delivery based on either criterion gives similar outcome. We will conduct more SLE pregnancies case studies to verify this result.

References

Adamson, S. L.; Morrow, R. J.; Langille, B. L.; Bull, S. B.; and Ritchie, J. W. K. 1990. Site-dependent effects of increases in placental vascular resistance on the umbilical arterial velocity waveform in fetal sheep. *Ultrasound in Medicine & Biology* 16(1):19–27.

Baschat, A. A.; Gembruch, U.; and Harman, C. R. 2001. The sequence of changes in doppler and biophysical parameters as severe fetal growth restriction worsens. *Ultrasound in Obstetrics and Gynecology* 18:571–577.

Clowse, M. E.; Magder, L. S.; Witter, F.; and Petri, M. 2006. Early risk factors for pregnancy loss in lupus. *Obstetrics & Gynecology* 107–293.

Ebbing, C.; Rasmussen, S.; and Kiserud, T. 2007. Middle cerebral artery blood flow velocities and pulsatility index and the cerebroplacental pulsatility ratio: longitudinal reference ranges and terms for serial measurements. *Ultrasound in Obstetrics and Gynecology* 30(3):287–296.

Eden, A. 1992. *The search for Christian Doppler*. Springer-Verlag.

Ferrazzi, E.; Bozzo, M.; Rigano, S.; Bellotti, M.; Morabito, A.; Pardi, G.; Bettaglia, F. C.; and Galan, H. L. 2002. Temporal sequence of abnormal doppler changes in the periph-

eral and central circulatory systems of the severely growth-restricted fetus. *Ultrasound in Obstetrics and Gynecology* 19:140–146.

Giles, W. B.; Trudinger, B. J.; and Baird, P. J. 1985. Fetal umbilical artery flow velocity waveforms and placental resistance: pathological correlation. *Br J Obstet Gynaecol* 92:31–38.

Guzman, E. R.; Vintzileos, A. M.; Martins, M.; Benito, C.; Houlihan, C.; and Hanley, M. 1996. The efficacy of individual computer heart rate indices in detecting acidemia at birth in growth-restricted fetuses. *Obstetrics & Gynecology* 87:969–974.

Holland, J. 1975. *Adaptation in Natural and Artificial Systems*. University of Michigan Press, Ann Arbor.

Jacob, C. 2001. *Illustrating Evolutionary Computation with Mathematica*. Morgan Kaufmann.

Marsal, K.; Laurin, J.; Lindblad, A.; and Lingman, G. 1987. Blood flow in the fetal decending aorta. *Seminars in Perinatology* 11(4):322–334.

Merz, E. 2004. *Ultrasound in Gynecology and Obstetrics, Second edition*. Thieme Medical Publishers.

Pardi, G.; Cetin, I.; Marconi, A. M.; Lanfranchi, A.; Bozzetti, P.; Ferrazzi, E.; Buscaglia, M.; and Battaglia, F. C. 1993. Diagnostic value of blood sampling in fetuses with growth retardation. *New England Journal of Medicine* 328:692–696.

Reed, K. L.; Appleton, C. P.; Anderson, C. F.; Shenker, L.; and Sahn, D. J. 1990. Doppler studies of vena cava flows in human fetuses. insights into normal and abnormal cardiac physiology. *Circulation* 81:498–505.

Romero, R.; Kalache, K. D.; and Kadar, N. 2002. Timing the delivery of the preterm severely growth-restricted fetus: venous doppler, cardiotocography or the biophysical profile. *Ultrasound in Obstetrics and Gynecology* 19:118–121.

Street, P.; Dawes, G. S.; Moulden, M.; and Redman, C. W. G. 1991. Short term variation in abnormal antenatal fetal heart rate records. *American Journal of Obstetrics and Gynecology* 165:515–523.

van den Wijngaard, J. P. H.; Westerhof, B. E.; Faber, D. J.; Ramsay, M. M.; Westerhof, N.; and Gemert, M. J. C. V. 2006. Abnormal arterial flows by a distributed model of the fetal circulation. *American Journal of Physiology Regulatory, Integrative and Comparative Physiology* 291:R1222–R1233.

Vintzileos, A. M.; Campbell, W. A.; and Rodis, J. F. 1989. Fetal biophysical profile scoring: current status. *Clin Perinatol* 16:661–689.

Waldimiroff, J. W.; van der Wijngaard, J. A.; Degani, S.; Noordam, M. J.; van Eyck, J.; and Tonge, H. M. 1987. Cerebral and umbilical arterial blood flow velocity waveforms in normal and growth-retarded pregnancies. *Obstetrics & Gynecology* 69:705–709.